

## Muon trapping at monovacancies in iron

A. Möslang, H. Graf, G. Balzer,\* E. Recknagel, A. Weidinger, and Th. Wichert  
*Physics Department, University of Konstanz, D-7750 Konstanz, Germany*

R. I. Grynspan  
*Centre d'Etudes de Chimie Métallurgique, F-94400 Vitry, France*  
 (Received 9 November 1982)

Positive-muon—spin-rotation experiments were performed on electron irradiated iron. A new defect-associated frequency is observed which is assigned to muons trapped at monovacancies. The hyperfine field at the vacancy site is  $-0.956$  T at 140 K. The diffusion constant for  $\mu^+$  in iron deduced from the trapping rate follows an Arrhenius law with an activation energy of  $38 \pm 3$  meV between 90 and 190 K.

### I. INTRODUCTION

In this paper we report on the direct observation of positive-muon trapping at lattice defects in electron-irradiated iron. The capture of the muons by the defects is evidenced by a change in the precession frequency of the muon spin. The underlying process is the following: Positive muons implanted into iron come to rest at an interstitial site and the spin starts precessing with the well-known frequency of about 50 MHz corresponding to the local magnetic field at an interstitial site in ferromagnetic Fe. Since the muons are highly mobile in Fe, they diffuse through the sample and may encounter defects where they are trapped. The trapping will in general change the precession frequency since the local field is different at the new position compared to the old one. For fast trapping, the change of the frequency can be seen directly in the muon—spin-rotation ( $\mu$ SR) time spectra.

Muon trapping at lattice defects has been reported before for various Al and Nb samples.<sup>1-4</sup> Since these materials are diamagnetic, the trapping does not show up in a change of the precession frequency, but rather in an increase of the relaxation rate. An advantage of the present experiment using a magnetic material for these studies lies in the fact that frequencies can be measured with much higher precision than relaxation rates and that therefore a clear distinction between different defects (trapping centers) is possible. Preliminary data of the present experiment were reported at two conferences.<sup>5,6</sup>

### II. EXPERIMENTAL DETAILS

The  $\mu$ SR experiment was performed at the low-momentum (28.8-MeV/c) muon beam at the Swiss

Institute for Nuclear Research (Schweizerisches Institut für Nuklearforschung) in zero external magnetic field. A general description of the  $\mu$ SR technique is given, e.g., in Ref. 7. Single-crystal Fe targets with an area of about 2 cm<sup>2</sup> and 1.8 mm thickness were used. The main impurities in the sample were 6.5 wt. ppm Si, 8.5 wt. ppm Al, and less than 6 wt. ppm Ni, all other contaminations being  $< 1$  wt. ppm. The targets were irradiated at 10 K with 3-MeV electrons at the Kernforschungsanlage Jülich. The irradiation doses were  $2.9 \times 10^{18}$  and  $7.3 \times 10^{18}$  e<sup>-</sup>/cm<sup>2</sup>. In addition, some data points around 220 K were taken with a sample irradiated with  $11 \times 10^{18}$  e<sup>-</sup>/cm<sup>2</sup>. The targets were loaded at 77 K into the  $\mu$ SR cryostat without being allowed to warm up above 90 K. The resistivity recovery was measured parallel to the  $\mu$ SR experiments.

Owing to the small range of the low-momentum muon beam it is assured that the muons are stopped in a homogeneously damaged layer. The  $\mu^+$  stopping rate was  $4 \times 10^4$  s<sup>-1</sup> and in each spectrum about  $10^7$  events were accumulated. An isochronal annealing program was performed *in situ* for 10 min at annealing temperatures  $T_A$ .  $\mu$ SR experiments were carried out at different measuring temperatures  $T_M$  well below  $T_A$ , so that no significant recovery took place during the experiment.

### III. RESULTS AND DISCUSSION

In Fig. 1  $\mu$ SR time spectra for four different temperatures  $T_M$  are shown. For all spectra, the annealing temperature  $T_A$  was 188 K. In the upper spectrum only one precession signal with a frequency  $\nu_1$  of about 50 MHz is observed. This signal is well known from experiments on unirradiated Fe samples and is attributed to muons diffusing over interstitial

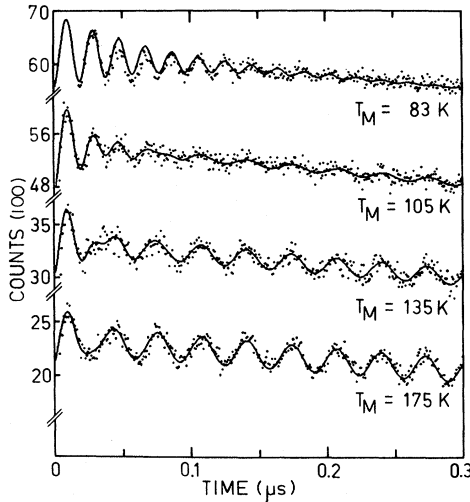


FIG. 1.  $\mu$ SR spectra of electron-irradiated iron annealed at  $T_A = 188$  K. At  $T_M = 83$  K only the well-known 50-MHz precession of interstitial muons in iron is seen. At higher temperature a second frequency (30 MHz) shows up after 10–70 ns. The transition from 50 to 30 MHz is a direct indication of muon trapping at vacancies after a certain mean free-diffusion time.

sites. In the lower spectra this frequency is observed only at the very beginning whereas after a short time a different frequency  $\nu_2$  of about 30 MHz shows up. This change in frequency is a direct indication that muons are trapped at defects. It is clearly seen that the trapping occurs in about 10–70 ns after the muon has entered the sample at  $t = 0$ . The time the muon needs to reach the defects decreases with increasing temperatures since the muons become more mobile. This shift towards shorter times increases the amplitude  $A_2$  of the second frequency since less dephasing occurs for shorter capture times. The solid lines in Fig. 1 are fits to the data with the expression

$$N(t) = N_0 \exp(-t/\tau_\mu) [1 + P(t)] + B, \quad (1)$$

with

$$P(t) = \sum_{i=1}^2 A_i \exp(-\lambda_i t) \cos(\omega_i t + \varphi_i).$$

Here  $\tau_\mu = 2.19 \mu\text{s}$  is the muon lifetime and  $B$  the background.  $A_i$ ,  $\lambda_i$ ,  $\omega_i$ , and  $\varphi_i$  are the amplitude, the relaxation rate, the frequency, and the phase, respectively. Index 1 is used for the free-diffusing component (50-MHz line) and index 2 for the trapped component (30-MHz line).

In Fig. 2 Fourier transforms of three characteristic  $\mu$ SR spectra are shown. Figure 2(a) shows the frequency spectrum from a measurement of an irradiated sample at  $T_M = 176$  K. One precession fre-

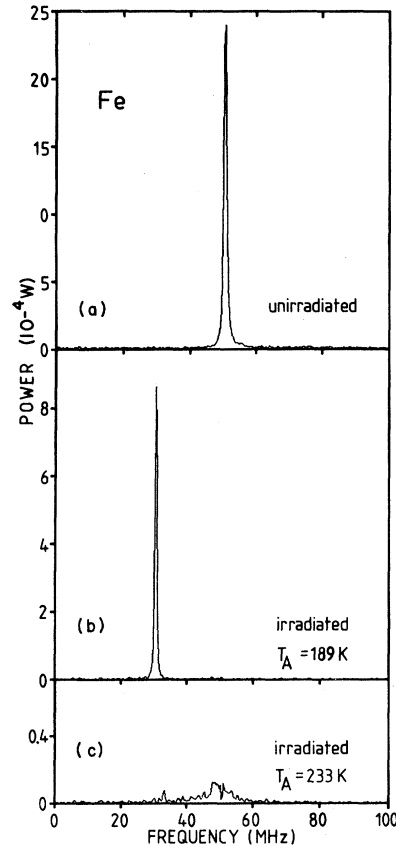


FIG. 2. Fourier transforms of  $\mu$ SR spectra over 1700 ns for unirradiated [Fig. 2(a)] and irradiated [Figs. 2(b) and 2(c)] iron samples. The measuring temperature was 176 K in all three cases. In Fig. 2(c) the sample was annealed above stage III (220 K) where monovacancies disappear.

quency at  $\nu_1 = 50$  MHz with a small linewidth is observed. In Fig. 2(b) the frequency spectrum of an irradiated sample annealed at  $T_A = 189$  K and measured at 176 K is shown. The signal with  $\nu_1 = 50$  MHz is not seen any more but a new frequency with  $\nu_2 = 30$  MHz shows up very clearly. This frequency is attributed to muons trapped at a defect. The small linewidth of the second frequency indicates that no detrapping occurs during the muon lifetime. At higher annealing temperatures ( $T_A = 233$  K) the frequency  $\nu_2$  is no longer observed [Fig. 2(c)]. Obviously the trapping centers disappeared during the annealing process. In Fig. 2(c) the signal at 50 MHz is still much broader than in the unirradiated sample. This indicates that some damage remained in the sample. Full recovery, i.e., a spectrum as seen in Fig. 2(a), is obtained after annealing at 1100 K. In the following, four aspects of the experiment (defect assignment, defect recovery, muon diffusion, and hyperfine fields) will be discussed separately.

### A. Defect assignment

An important result of the present experiment is the fact that only *one* defect line is observed experimentally (Fig. 2). The large intensity of this line which exhausts the expected strength almost completely excludes the possibility that strong lines in unobserved frequency regions could have been overlooked.

The observation of a single defect line implies, first of all, that only *one* major type of trapping center can exist in the sample. In addition the trapping center must be simple since complex defects would not give a unique configuration. Therefore, in the following, only monovacancies, divacancies, and monointerstitials will be considered further.

Interstitial defects can be excluded by the following arguments: Monointerstitials at tetrahedral or octahedral sites and  $\langle 100 \rangle$  dumbbells have tetragonal symmetry with the symmetry axis along the cube axes. Since these axes can be either parallel or perpendicular to the  $\langle 100 \rangle$  magnetization direction, they would give rise to magnetically inequivalent configurations and therefore would cause a splitting of the line. This splitting should be in the order of a few MHz, corresponding to typical dipolar fields in Fe, and therefore should be easily detectable. A similar argument holds for the  $\langle 110 \rangle$  dumbbell which is considered as the stable interstitial configuration in Fe.<sup>8-10</sup> Since no splitting is observed experimentally, these configurations can be excluded. The only simple interstitial defect consistent with the observation of a single line is the  $\langle 111 \rangle$  dumbbell. However, there is neither experimental<sup>8,9</sup> nor theoretical<sup>10</sup> evidence for the existence of such a configuration in Fe. Therefore, the 30-MHz line cannot be attributed to muons trapped at interstitial defects.

Among the divacancy configurations again, only those with a  $\langle 111 \rangle$  symmetry axis are acceptable on the basis of symmetry considerations. However, model calculations<sup>10</sup> indicate that these configurations are not stable in bcc metals, but the main argument against a divacancy assignment comes from a consideration of the defect production process in  $e^-$ -irradiated samples. Whereas it seems completely plausible that monovacancies dominate in  $e^-$ -irradiated samples, the opposite, namely a dominance of divacancies, seems rather unrealistic. It should be emphasized that the present experiment is an exclusive one; i.e., if the 30-MHz line is assigned to divacancies then there can be no trapping at monovacancies. Although the production of divacancies is possible with 3-MeV electrons, it seems nevertheless completely unrealistic to assume that *only* divacancies are produced. An explanation of

the data with extremely different trapping radii or binding energies of monovacancies and divacancies for muons seems not very satisfactory either. Therefore, we conclude that the 30-MHz line has to be attributed to muons trapped at monovacancies.

The monovacancy assignment gives a completely satisfactory explanation of the data. In particular, no additional lines are expected since (i) the number of the other defects is rather small, and (ii) most of them produce a splitting of the line reducing the intensity in each one of them. On the other hand, the monovacancy has cubic symmetry and therefore the whole intensity is contained in a single line.

Before proceeding, the possibility of an off-center position of the trapped muon should be considered. If static, the off-center position would again produce a splitting of the line and therefore can be ruled out on the basis of the experimental observation. However, an off-center position with a fast motion of the muon around the substitutional site would be in complete accordance with the present experiment. Assuming dipolar fields at the off-center position in the order of 0.1 T (typical values in Fe), a hopping rate larger than a few times  $10^{10}$  per second would be required in order to average out the dipolar splitting to less than the observed linewidth of 0.3 MHz. Muon hopping rates in this order of magnitude are not unreasonable in this temperature range.<sup>11</sup> Therefore, the substitutional and the off-center position of the muon cannot be distinguished by the present experiment.

It should be mentioned that a fast motion of the muon around a defect which by itself has noncubic symmetry would not avoid a splitting of the defect line. Therefore, the argument used above to exclude the interstitial assignment remains valid even if the muon performs jumps around this defect.

### B. Defect recovery

Figure 3 shows the amplitude of the 30-MHz defect line as a function of the annealing temperature for two different measuring temperatures. It is seen that the defect line disappears in recovery stage III around 220 K. In an especially designed experiment with high irradiation dose ( $11 \times 10^{18} e^-/\text{cm}^2$ ) and high counting statistics [Figs. 2(b) and 2(c)] it was found that the amplitude of the defect line goes down in stage III at least by a factor of 35, indicating a drastic reduction (or complete annealing) of monovacancies. This result has to be confronted with a resistivity recovery in stage III of only a factor of 5.<sup>12</sup> According to the two-interstitial model,<sup>13</sup> monovacancies disappear in stage III by recombination with mobile interstitials; therefore, the reduction of the monovacancy concentration should not

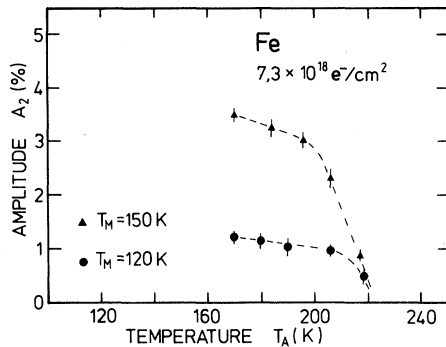


FIG. 3. Amplitude  $A_2$  of the defect line (30 MHz) as function of the annealing temperature  $T_A$ . The  $\mu$ SR measurements were performed at  $T_M=120$  and 150 K, respectively. The sample was irradiated with  $7.3 \times 10^{18} e^-/\text{cm}^2$ .

be larger than of the resistivity, i.e., a factor of 5 or less. However, a reduction of the monovacancy concentration of only a factor of 5 is not consistent with the complete disappearance of the defect line in the present experiment. Therefore, the two-interstitial model cannot be accepted for Fe.

A natural explanation of both the  $\mu$ SR and resistivity results is obtained if one assumes that vacancies migrate in stage III. In this model,<sup>14</sup> monovacancies disappear completely in stage III either by recombination or by clustering, whereas some resistivity from clusters remains in the sample. This is apparently in agreement with the data. Monovacancy migration at 220 K was postulated also by Vehanen *et al.*<sup>15</sup> from a positron annihilation experiment but a different interpretation of the data was given by Frank *et al.*<sup>16</sup>

The general recovery of the sample by defect annealing shows up also in the relaxation rate  $\lambda_1$  of the free-diffusing muon component (50-MHz line). The behavior of  $\lambda_1$  as a function of the annealing temperature (Fig. 4) resembles strongly the resistivity recovery curves obtained in Ref. 12: Stage I at 110 K and stage III at 220 K are clearly seen in Fig. 4. Full recovery, i.e., a  $\lambda_1$  value as in the unirradiated sample, requires annealing above 1100 K.

### C. Muon diffusion

Figure 5 shows Fourier spectra for the same annealing but for different measuring temperatures. The change of the intensity from the 50- to the 30-MHz line and the increase of the 30-MHz line with increasing temperature is clearly seen. From this behavior the following picture has evolved: We assume that muons implanted into the target stop randomly at interstitial sites, in general, in an undisturbed lattice area. From this point on the muons

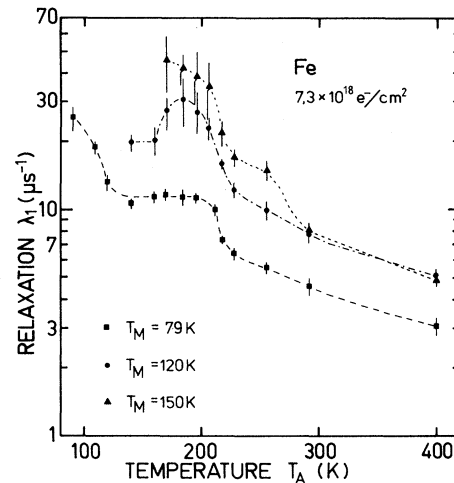


FIG. 4. Relaxation rate  $\lambda_1$  of the 50-MHz line as a function of the annealing temperature  $T_A$ . The measuring temperatures  $T_M$  were 79, 120, and 150 K, respectively.

start diffusing through the crystal while the spin is precessing with 50 MHz. If trapped at a monovacancy at time  $t'$  the precession frequency changes suddenly from 50 to 30 MHz; therefore, for an indi-

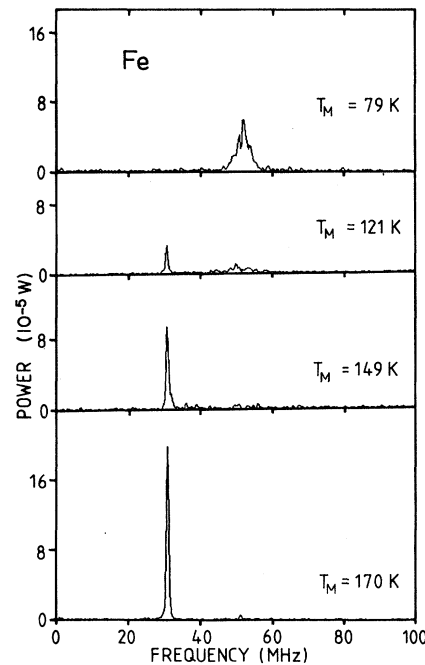


FIG. 5. Fourier transforms of  $\mu$ SR spectra on irradiated iron. The annealing temperature  $T_A$  was 206 K for all four runs but the measuring temperature  $T_M$  was changed. At  $T_M=79$  K only the 50-MHz line of muons at interstitial sites is seen. With increasing temperature the muons become more mobile and reach the defects faster with the consequence that the intensity of the 30-MHz line increases.

vidual muon the polarization  $P(t)$  has the following form:

$$P(t) = A_0 \Theta(t-t') \cos \omega_1 t + A_0 \Theta(t-t') \times \cos[\omega_2(t-t') + \omega_1 t'], \quad (2)$$

$$P(t) = A_0 e^{-t/\tau_D} \cos(\omega_1 t) + \frac{A_0}{[1 + (\Delta\omega\tau_D)^2]^{1/2}} \cos(\omega_2 t + \arctan(\Delta\omega\tau_D)) - \frac{A_0}{[1 + (\Delta\omega\tau_D)^2]^{1/2}} e^{-t/\tau_D} \cos(\omega_1 t + \arctan(\Delta\omega\tau_D)), \quad (3)$$

where  $\tau_D$  is the mean free-diffusion time before trapping,  $A_0$  is the initial amplitude (15.5%), and  $\Delta\omega = \omega_1 - \omega_2$  is the difference between the precession frequencies in the free and trapped states, respectively. Comparison of formulas (1) and (3) shows that the parameters of the first frequency (index 1) are determined by the first and third term in (3), and those of the second frequency (index 2) by the second term in (3). Formula (3) is derived assuming one kind of trapping center only and no intrinsic relaxation. Modification including these effects will be discussed together with the interpretation of the data.

It can be seen from formula (3) that the interesting quantity  $\tau_D$  is contained in three independent experimental parameters: (i) the relaxation rate  $\lambda_1$ , (ii) the amplitude  $A_2$ , and (iii) the phase  $\varphi_2$ . In the following, these quantities will be discussed in more detail.

The relaxation rate  $\lambda_1$  of the 50-MHz line is shown in Fig. 6 as a function of temperature; the different curves refer to different annealing temperatures. It can be seen that in the whole temperature range  $\lambda_1$  is appreciably larger for the irradiated than for the unirradiated sample. In general, a V-shape behavior with a minimum around 60–100 K is observed. We think that the differences in  $\lambda_1$  at the low temperatures ( $T < 60$  K) are caused mainly by the lower mobility of the muon in the disturbed lattice. Since the low-temperature region is dominated by quantum diffusion, strain fields from defects are expected to have a large effect on the mobility of the muon. Note that the minimum of  $\lambda_1$  at 15 K is smeared out in the irradiated sample. This behavior is expected if one assumes that the coherent tunneling process proposed for  $T_M < 35$  K in Ref. 11 is especially influenced very strongly by defects.

The reincrease of  $\lambda_1$  above 60 K is closely connected with the muon trapping at defects. One contribution to  $\lambda_1$  comes from the term  $1/\tau_D$  in formula (3). However, there are additional terms in  $\lambda_1$  which originate from the intrinsic relaxation and

where  $\Theta(t-t') = 1$  for  $t-t' > 0$  and  $\Theta(t-t') = 0$  otherwise.

The behavior of the muon ensemble is obtained by integrating (2) over the trapping time  $t'$  with the weighting function  $1/\tau_D \exp(-t'/\tau_D)$ . The result is

from trapping at other defects. Therefore,  $\lambda_1$  gives only an upper limit for  $1/\tau_D$ . In the interesting region, the experimental value of  $\lambda_1$  was found to be about twice as large as  $1/\tau_D$  derived from the amplitude  $A_2$  (see below). The difference between  $\lambda_1$  and  $1/\tau_D$  must be attributed to lower mobility of the muon in the disturbed lattice and to trapping (with possible detrapping) at other defects.

The amplitude  $A_2$  of the second frequency is shown in Fig. 7 as a function of temperature. The data points above 150 K were taken after partial annealing of the sample; in the analysis, these data points were corrected for the annealing effect via measurements at 150 K where runs were made be-

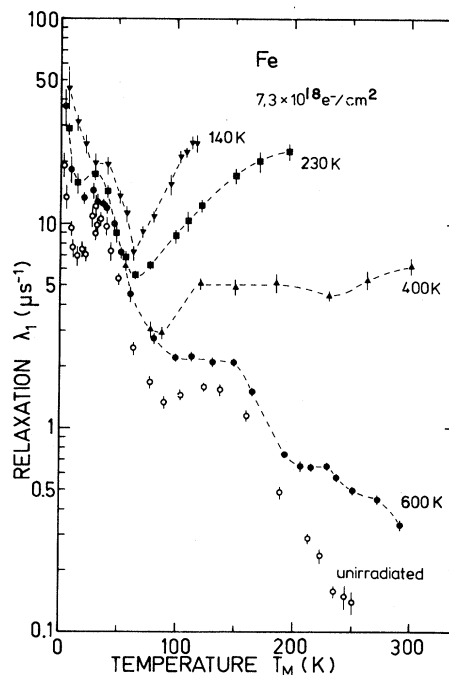


FIG. 6. Relaxation rate  $\lambda_1$  of the 50-MHz line as a function of the measuring temperature  $T_M$  for different annealing temperatures  $T_A$ .

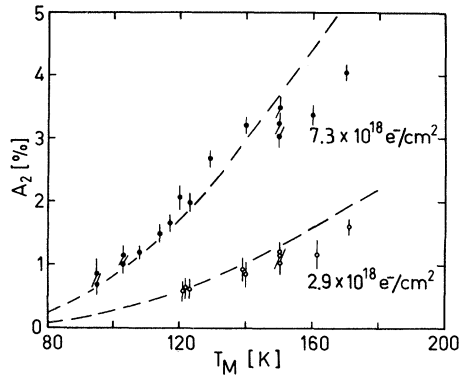


FIG. 7. Amplitude  $A_2$  of the 30-MHz line as a function of temperature for two different irradiation doses. The dashed lines are obtained assuming an Arrhenius law for the diffusion coefficient. The data points above 150 K were measured after partial annealing of the sample.

fore and after annealing. From  $A_2$  the mean free-diffusion time  $\tau_D$  can be extracted using the relation  $A_2 = A_0 [1 + (\Delta\omega)^2 \tau_D^2]^{-1/2}$ . Since  $\Delta\omega$  is known experimentally (the sign of  $\omega_1$  and  $\omega_2$  were determined by applying an external field), the only uncertainty in  $A_2$  is due to  $A_0$  which in a real experiment might be smaller than the initial amplitude of 15.5%. A possible reduction would be due to other trapping centers in addition to the one considered here. However, a fit of  $A_2$  with an Arrhenius function for  $\tau_D$  as a function of temperature indicates that  $A_0$  is close to the initial amplitude of 15.5%. Therefore, in the final analysis  $A_0$  was fixed at 15.5%. The values of  $\tau_D$  obtained from the  $A_2$  analysis were used in the calculation of the diffusion constant.

Finally,  $\tau_D$  can be extracted from the phase shift  $\varphi_2$  via the relation  $\varphi_2 = \arctan(\Delta\omega \tau_D)$ . Since  $\varphi_2$  contains no unknown factors, it would be in principle the most suited parameter for the determination of  $\tau_D$ . Unfortunately, the phase shift is very insensitive to  $\tau_D$  in the experimentally important region of  $\Delta\omega \tau_D \gg 1$ , where  $\varphi_2$  is close to  $\pi/2$ . However, this part is covered safely by the  $A_2$  analysis. In the critical region, where  $\Delta\omega \tau_D$  comes close to 1, the experimental value of  $\varphi_2$  is consistent with  $\tau_D$  derived from  $A_2$ .

The mean free-diffusion time  $\tau_D$  measured in the present experiment can be used to derive the diffusion coefficient of muons in Fe. Assuming diffusion-limited trapping and some additional simplifications, the following relation holds<sup>17</sup>:

$$1/\tau_D = c_v \frac{4\pi r_v}{V_A} D_\mu, \quad (4)$$

where  $r_v$  is the trapping radius of the vacancy and  $V_A$  the atomic volume. The vacancy concentration

$c_v$  was determined from the measured resistivity assuming  $\Delta\rho_{FP} = 3.0 \times 10^{-11} \Omega\text{m}$  per ppm Frenkel pair (FP).<sup>18</sup> The resistivity recovery measured parallel to the  $\mu\text{SR}$  measurements was in good agreement with that reported in Ref. 12. In the temperature range above stage I (110 K) but below stage III (220 K) we obtain a vacancy concentration of 19 ppm for the high and 7 ppm for the low irradiation dose. For the trapping radius,  $r_v = 3a$  ( $a$  is the lattice constant) was assumed. A value of this order of magnitude is suggested from measurements of the spontaneous recombination volume of Frenkel defects in irradiated bcc metals.<sup>19</sup>

The diffusion coefficient  $D_\mu$  obtained from Eq. (4) using  $\tau_D$  from the  $A_2$  analysis is plotted in Fig. 8 as a function of inverse temperature. A fit with an Arrhenius law (dashed line in Fig. 8) yields an activation energy  $E_a = 38 \pm 3$  meV and a preexponential factor  $D_0 = (3.3 \pm 0.3) \times 10^{-4} \text{ cm}^2/\text{s}$ . The errors account for statistical uncertainties only. In addition,  $D_0$  may have systematic error (factor of 3–5) since  $c_v$  and  $r_v$  are not well known. Using the parameters given above the dashed lines in Fig. 7 displaying the temperature and dose dependence of the amplitude  $A_2$  were obtained.

Muon diffusion in unirradiated iron was studied in earlier experiments<sup>11,20,21</sup> by the motional narrowing method. The data of the different groups agree fairly well below 90 K, but larger discrepancies occur at higher temperatures. It was shown<sup>20,21</sup> that above 90 K the  $\lambda$  values of Ref. 11 are influenced by impurities; therefore, in the following, the data of Ref. 20 will be considered.

The present results are in excellent agreement

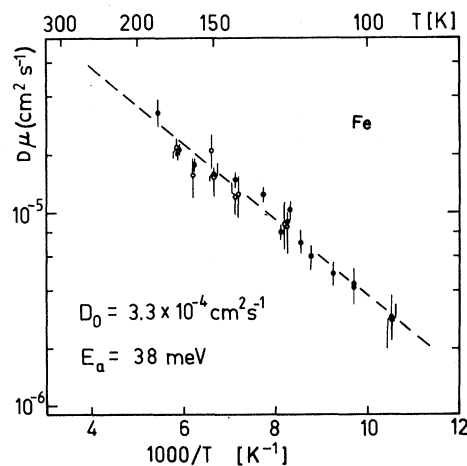


FIG. 8. Diffusion coefficient  $D_\mu$  for positive muons in iron calculated from the trapping rate at vacancies. Open and closed circles are for the low and high dose irradiation (7 and 19 ppm vacancies below stage III), respectively.

with the motional narrowing data<sup>20</sup> if diffusion over tetrahedral interstitial sites is assumed whereas a discrepancy of a factor of 26 occurs for diffusion over octahedral sites (the large difference is caused mainly by the different dipolar fields at these sites). Although this discrepancy is rather large, no firm exclusion of octahedral occupancy can be made since the argument relies on the absolute value of  $D_0$  and on the calculated dipolar fields, i.e., on quantities which are not well known. But in spite of these uncertainties, a preference for the tetrahedral occupancy of the muon is suggested.

#### D. Hyperfine field

In zero external field the local magnetic field  $B_\mu$  and the hyperfine field  $B_{\text{hf}}$  at the muon site can be calculated from the measured frequency  $\nu_2$  by the following formulas:

$$B_\mu = 2\pi\nu_2/\gamma, \quad (5)$$

$$B_{\text{hf}} = B_\mu - \frac{4\pi}{3}M_S.$$

Thereby, the dipolar field contribution was neglected because of the cubic symmetry discussed above.  $\gamma$  is the gyromagnetic ratio and  $M_S$  the saturation magnetization;  $M_S$  was calculated as  $M_S = \rho(T)\sigma_{\text{st}}$ , where  $\sigma_{\text{st}}$  is the saturation magnetization per unit mass at temperature  $T$  (taken from Ref. 22), and  $\rho(T)$  is the sample density. The density as a function of temperature was calculated assuming  $\rho(293 \text{ K}) = 7.874 \text{ g/cm}^3$  and using the temperature-dependent lattice parameters of Ref. 23.

Figure 9 shows the measured frequencies  $\nu_2$  in the upper part and the derived hyperfine field  $B_{\text{hf}}$  in the lower part. The solid line represents the saturation magnetization  $M_S$  normalized to  $B_{\text{hf}}$  at  $T = 183 \text{ K}$ . The experimental data are limited at the low-temperature side by the fact that the muons are too slow and do not reach the defect in a sufficient short time and on the high-temperature side by the annealing of monovacancies in stage III around 220 K.

The hyperfine field (Fig. 9) shows an unusual temperature dependence with an increase of  $B_{\text{hf}}$  between 90 and 140 K. This increase is not well understood at present. In principle, two explanations are conceivable: (i)  $B_{\text{hf}}$  directly reflects the temperature dependence of the local magnetic field in Fe, or (ii) the spatial extension of the muon wave function changes with temperature, with the consequence that the muon averages over different regions in the crystal when the temperature is changed. The second explanation seems to be a more likely one to us.

Assuming that the increase of  $B_{\text{hf}}$  around 100 K

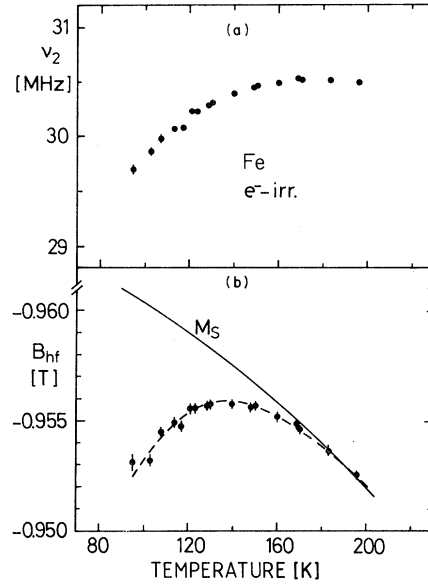


FIG. 9. (a) Precession frequency of trapped muons as a function of temperature. (b) Hyperfine field  $B_{\text{hf}}$  calculated from the measured frequencies. The solid line shows the relative temperature dependence of the saturation magnetization  $M_S$  normalized at 183 K.

is due to the thermal population of an excited state of the muon, a level energy on the order of 10 meV would be suggested. Such low-lying states are very likely to be due to tunneling splittings, but vibrational states in a very flat potential are also possible.

An alternative explanation would be a hopping model where the muon changes places between the substitutional and neighboring interstitial sites. Assuming that the hyperfine field at the interstitial site is close to the value of the undisturbed lattice, i.e., on the order of  $-1.1 \text{ T}$ , and at the substitutional site close to zero,<sup>24,25</sup> then a weighted average of  $B_{\text{hf}} = -0.95 \text{ T}$  may well be obtained. In this model, the increase of  $B_{\text{hf}}$  around 100 K could be explained by assuming that the mean time of residence of the muon changes slightly from the substitutional to the interstitial sites when the temperature is raised. However, this model should not be taken too literally since the muon is certainly not well localized and therefore local considerations are not very realistic.

The muon hyperfine field at the substitutional site was calculated by Kanamori *et al.*<sup>24</sup> and Akai *et al.*,<sup>25</sup> and was found to be close to zero. However, these authors claim that the total energy favors an off-center position of the muon and that at these places the field is indeed strongly negative with values in reasonable agreement with the experimental result. Estreicher and Meier<sup>26</sup> calculated  $B_{\text{hf}}$  values between  $-0.6$  and  $-0.9 \text{ T}$  in a model where

lattice and muon vibrations were included explicitly. From these calculations,<sup>24-26</sup> it seems obvious, that extended wave functions and/or off-center positions of the muon are required to explain the data on the hyperfine field.

#### IV. CONCLUSION

Muon trapping at monovacancies in iron was observed. The trapping shows up in a very direct way as a change of the precession frequency in the time spectrum. The high sensitivity of the frequency measurement makes it possible to study this process

well separated from other events which might occur in parallel. Detailed results were obtained for (a) the defect annealing, (b) the muon diffusion in Fe, and (c) the hyperfine field at the vacancy site.

#### ACKNOWLEDGMENTS

The financial support of the Bundesminister für Forschung und Technologie is gratefully acknowledged. We thank Dr. Dworschak and Professor Schilling of the Kernforschungsanlage Jülich for the electron irradiations.

\*Present address: Physics Department, University of Dortmund, D-4600 Dortmund, Germany.

- <sup>1</sup>W. J. Kossler, A. T. Fiory, W. F. Lankford, J. Lindemuth, K. G. Lynn, S. Mahajan, R. P. Minnich, K. G. Petzinger, and C. E. Stronach, *Phys. Rev. Lett.* **41**, 1558 (1978).
- <sup>2</sup>M. Doyama, R. Nakai, H. Fukushima, N. Nishida, Y. J. Uemura, and T. Yamazaki, *Hyperfine Interact.* **6**, 341 (1979).
- <sup>3</sup>J. A. Brown, R. H. Heffner, M. Leon, M. E. Schillaci, D. W. Cooke, and W. B. Gauster, *Phys. Rev. Lett.* **43**, 1513 (1979).
- <sup>4</sup>K. Dorenburg, M. Gladisch, D. Herlach, W. Mansel, H. Metz, H. Orth, G. zu Putlitz, A. Seeger, W. Wahl, and M. Wigand, *Z. Phys. B* **31**, 165 (1978); D. Herlach, in *Recent Development in Condensed Matter Physics*, edited by J. C. Devreese (Plenum, New York, 1981), Vol. 1, p. 93.
- <sup>5</sup>A. Möslang, H. Graf, E. Recknagel, A. Weidinger, Th. Wichert, and G. I. Grynspan, in *Yamada Conference V on Point Defects and Defect Interactions in Metals*, edited by J. Takamura, M. Doyama, and M. Kiritani (University of Tokyo Press, Tokyo, 1982), p. 11.
- <sup>6</sup>H. Graf, A. Möslang, E. Recknagel, and A. Weidinger, in *Proceedings of the International Symposium on the Electronic Structure and Properties of Hydrogen in Metals*, edited by P. Jena (Plenum, New York, in press).
- <sup>7</sup>A. Schenck, in *Nuclear and Particle Physics at Intermediate Energies*, edited by J. B. Warren (Plenum, New York, 1975), p. 159.
- <sup>8</sup>V. Hivert, R. Pichon, H. Bilger, P. Bichon, J. Verdone, D. Dautreppe and P. Moser, *J. Phys. Chem. Solids* **31**, 1843 (1970).
- <sup>9</sup>W. Chambron, J. Verdone and P. Moser, in *Fundamental Aspects of Radiation Damage in Metals*, edited by M. T. Robinson and F. W. Young, Jr. (US-ERDA-Conference 751006, 1975), p. 261.
- <sup>10</sup>R. A. Johnson, *Phys. Rev.* **134**, A1329 (1964).
- <sup>11</sup>H. Graf, G. Balzer, E. Recknagel, A. Weidinger, and R. I. Grynspan, *Phys. Rev. Lett.* **44**, 1333 (1980).
- <sup>12</sup>S. Takaki, J. Fuss, H. Kugler, U. Dedek, and H. Schultz, *Radiat. Effs.* (in press).
- <sup>13</sup>A. Seeger, in *Fundamental Aspects of Radiation Damage in Metals*, edited by M. T. Robinson and F. W. Young, Jr. (US-ERDA-Conference 751006, 1975), p. 493.
- <sup>14</sup>W. Schilling, P. Ehrhart, and K. Sonnenberg, in *Fundamental Aspects of Radiation Damage in Metals*, edited by M. T. Robinson and F. W. Young, Jr. (US-ERDA-Conference 751006, 1975), p. 470.
- <sup>15</sup>A. Vehanen, P. Hautojärvi, J. Johansson, J. Yli-Kaupilla, and P. Moser, *Phys. Rev. B* **25**, 762 (1982).
- <sup>16</sup>W. Frank, A. Seeger, and M. Weller, *Radiat. Eff.* **55**, 111 (1981).
- <sup>17</sup>A. Seeger, *Hyperfine Interact.* **6**, 313 (1979).
- <sup>18</sup>F. Maury, M. Biget, P. Vajda, A. Lucasson, and P. Lucasson, *Phys. Rev. B* **14**, 5303 (1976).
- <sup>19</sup>M. Biget, R. Rizk, P. Vajda, and A. Bessis, *Solid State Commun.* **16**, 949 (1975).
- <sup>20</sup>E. Yagi, H. Bossy, K. P. Döring, M. Gladisch, D. Herlach, H. Matsui, H. Orth, G. zu Pulitz, A. Seeger, and J. Vetter, *Hyperfine Interact.* **8**, 553 (1981).
- <sup>21</sup>A. Yaouanc, J. Chappert, O. Hartmann, L. O. Norlin, and E. Karlsson, *Hyperfine Interact.* **8**, 667 (1981).
- <sup>22</sup>J. Crangle and G. M. Goodman, *Proc. R. Soc. London Ser. A* **321**, 477 (1971).
- <sup>23</sup>*Thermophysical Properties of Mater.*, edited by Y. S. Touloukian (IFI/Plenum, New York, 1975), Vol. 12, p. 157.
- <sup>24</sup>J. Kanamori, H. K. Yoshida, and K. Terakura, *Hyperfine Interact.* **8**, 573 (1981).
- <sup>25</sup>M. Akai, H. Akai, and J. Kanamori, *J. Magn. Magn. Mater.* (in press).
- <sup>26</sup>S. Estreicher and P. F. Meier, *Phys. Rev. B* **25**, 297 (1982).